

Overview of Nanoparticle Project in Japan

Yukio Yamaguchi and Masahiro Fujita
*Department of Chemical System Engineering, School of Engineering,
The University of Tokyo, Hongo 7-3-1, Bunkyo-ku, Tokyo 113-8656, Japan*

The nanotechnology Particle Project (2001-2006, with K. Okuyama as project director and Y. Yamaguchi as deputy director) has been conducted as a part of the “nanotechnology Materials Program” founded by the METI.

Self-organization is a key concept for material science. Most of all issues on self-organization are related to a material processing. Collective properties also deeply depend on self-organization of electron, photon, phonon, and magnetic relating to the nanostructure of materials. We can control collective properties through the nanostructure of materials. In other words, nanostructure bridges function and process.

Various kinds of nanoparticles have been expected to explore new functions or to improve bulk properties as new materials (nanomaterials), which are a thin film or a composite. Since the physical properties of the nanomaterials are strongly affected by nano-interfaces existing among nanoparticles, the study of the nano-processing becomes crucial to design the nanomaterials. Here, we show two topics; (1) the fabrication of thin films of nanoparticles by wet coating, (2) the ordering of nanoparticles during drying.

INTRODUCTION

Nanomaterials such as a composite can improve physical characteristics of bulk materials. Thin films of nanoparticles have been expected to explore new characteristics based on nano-size physics. For instance, optical recording media, high density magnetic media, solar cells, and medical diagnostic devices are studied. We focus on the fundamental technology of nanoprocessing by fabricating the future devices above mentioned.

The key issue of nanofabrication is to control the self-assembly or the self-organization of nanoparticles. These concepts have been studied in many fields, but there are few studies on realistic industrial technology. Therefore, we have studied the self-alignment of nanoparticles by using conventional coating methods under high speeds and for wide area substrates which are indispensable for industrial applications.

1. Self-ordering of nanoparticles by wet coating⁽¹⁾

We investigate the effect of inter-particle repulsion and particle-substrate interaction on the microstructure of silica particle monolayer films fabricated by an evaporation-induced self-assembly method as a function of surface coverage. Suspensions of mono-dispersed colloidal silica particles (106nm diameter) without polymer binders cast on PET substrates by bar coating were dried under a controlled condition to obtain a two-dimensional particle film. The inter-particle repulsion was controlled by zeta potential of the particle suspensions. The particle-substrate interaction was also controlled by the surface treatment of substrates by argon radio frequency

plasma. The self-assembled microstructure was observed by atomic force microscopy and quantitatively evaluated by Voronoi analysis in terms of particle order and domain quality. In all the conditions attempted, the microstructure improves with the increase of Φ_C . However, little difference in the correlation between surface coverage (Φ_C) and the microstructure due to the experimental conditions was observed until Φ_C reached about 0.6, where both particle order and domain quality of more inter-particle repulsion (higher absolute value of zeta potential) began to exceed those of less inter-particle repulsion only when the substrates with less particle-substrate attraction (substrates with no surface treatment) were used. These results were consistent with the AFM observation. By considering a feasible model for the process, the microstructure dependence on the inter-particle repulsion most likely originate from a leap in the frequency of inter-particle collision at a critical value of Φ_C ($=49/75 \approx 0.65$ in the model). We found that stronger inter-particle repulsion and weaker particle-substrate attraction are preferable for the better microstructure above the critical Φ_C of about 0.6.

We define the coverage of the particle film as Φ_C ($= N/N_{fcc}$, where N , N_{fcc} represent the number of particle in the particle monolayer and the ideal fcc monolayer, in a unit area, respectively). Figure 1 shows Φ_C as a function of the particle weight fraction of the suspensions (Φ_{wp}).

Theoretically, if there is no size distribution of the particle and no occurrence of multilayer, Φ_C ($0 < \Phi_C < 1$) is represented as a function of Φ_{wp} by mass balance equation (1);

h : initial thickness of the liquid films ($=4.3\text{nm}$),

d_d : density of the dispersion medium ($=813\text{Kg m}^{-3}$, d_p : density of the particle ($=2100\text{Kg m}^{-3}$, D : average diameter of the particle ($=106\text{nm}$). The value of $\Phi_{wp}=0.0357$ corresponds to $\Phi_C=1$.

$$\phi_c = \frac{3\sqrt{3}hd}{\pi D} \times \frac{\phi_{wp}}{d_p + (d_d - d_p)\phi_{wp}} \quad (1)$$

In the experiment, when the Φ_{wp} excess 0.03 (corresponds to $\Phi_C > 0.86 \sim 0.88$), the correlation between Φ_{wp} and Φ_C begins to deviate from the equation (1) along with the emergence of bi-layer partially on the monolayer that is not yet completed. With the increase of Φ_{wp} , over 0.03, Φ_C increases along with the expansion of the deviation before Φ_C saturates around 0.91 ($\Phi_{wp}=0.035$). In this study we focus on the microstructure of the part of monolayer exclusively.

A comprehensive measure for the quantitative evaluation of the particle order is the fraction of particles with 6 nearest neighbors, in other words, the fraction of the polygons with 6 vertices among all polygons that constitute Voronoi diagram ($= \Phi_{VP6}$).

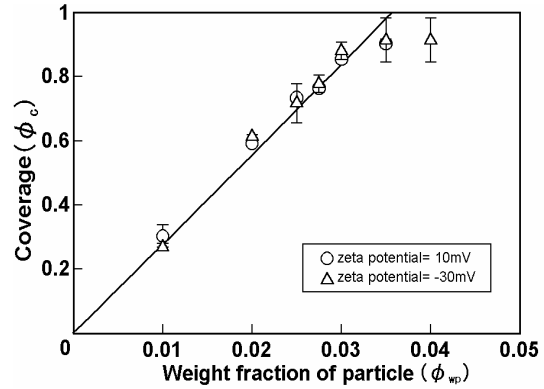


Figure 1 Coverage of the particle films (ϕ_c) as a function of particle weight fraction (ϕ_{wp}); the inset line represents the theoretical correlation between ϕ_c and ϕ_{wp} .

Figure 2 shows Φ_{VP6} as a function of Φ_C when substrates with no surface treatment were used. With the increase of Φ_C , Φ_{VP6} also increases in all cases alike until Φ_C reaches about 0.6 where the difference of the correlation between Φ_C and Φ_{VP6} due to zeta potential takes place. With further increase of Φ_C , the difference becomes larger. In the case of $\Phi_C > 0.6$, Φ_{VP6} of $\tilde{30mV}$ is larger than that of $10mV$. These results are consistent with the AFM observation (Figure 1). Thus the stronger inter-particle repulsion is preferable in terms of the particle order.

Figure 3 shows Φ_{VP6} as a function of Φ_C . When the more hydrophilic substrates are used, any difference in the correlation between Φ_C and Φ_{VP6} due to zeta potential does not occur at any range of Φ_C .

The increase in the hydrophilicity of the substrates due to the surface treatment is attributed

to the removal of contamination and increase in the number of hydrophilic group on the surface. The increased hydrophilicity should enhance the attraction between the substrate and particles which are abundant in hydrophilic silanol group on their surface. Therefore the mobility of the particles during the particle organization on the substrate should be retarded by the stronger particle-substrate attraction, which results in the less particle order.

2. Self-ordering of nanopartilces during drying⁽⁴⁾

A three-dimensional structure formation simulator of colloidal nanoparticles during drying is developed. Motion of the nanoparticles is modeled by Langevin equation, in which forces exerted on each nanoparticle consist of contact force, capillary force, Brownian force, van der Waals force, electrostatic force and fluid drag force. Drying of the colloid is described as a variation of interface between gas and liquid with time. The present simulator is applied to a drying process of a colloid film on a flat substrate, so that a multilayer structure of nanoparticles is formed. The structure formation is visualized with time, and the vertical structure and the planar structure of nanoparticles are quantitatively evaluated.

Capability of the present simulator is demonstrated by a drying simulation of a colloid film on a flat

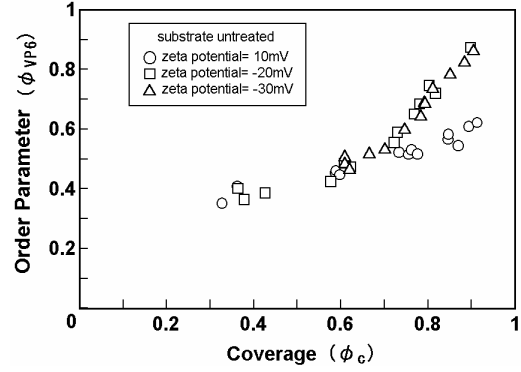


Figure 2. Order parameter (Φ_{VP6}) of the particle films as a function of coverage (Φ_C); the effect of zeta potential (no surface treatment).

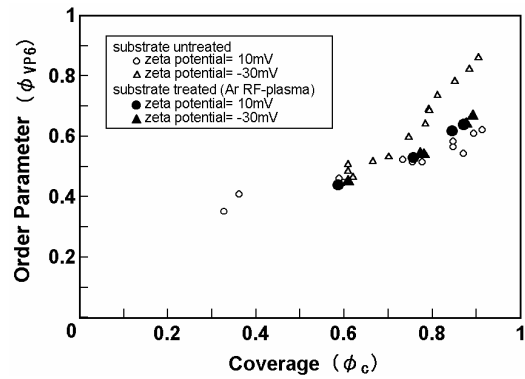


Figure 3. Order parameter (Φ_{VP6}) of the particle films as a function of coverage (Φ_C); the effect of surface treatment of substrates.

substrate. Computational conditions are chosen as follows: Width of the region is 1.35 mm and height is 150 nm that is equal to initial thickness of the colloid film. A periodic boundary condition is imposed on four vertical faces of the region. The volume fraction of colloidal nanoparticles is 0.4, in which the number of nanoparticles is 1683. In this case, the coverage ratio, which is equal to 1 when the computational region is covered with a monolayer of hexagonally close-packed nanoparticles, is 2. The diameter and the zeta potential of the nanoparticles are 50 nm and -50 mV, respectively. The temperature and the viscosity of the solvent are 20 °C and 0.001 Ns/m², respectively. The contact angle on the nanoparticles is 60°. The frictional coefficient between the nanoparticles and between the nanoparticles and the substrate are 0.2 and 0.02, respectively. The simulation time is 15 ms and the time step is 0.01ns.

In the case of computational conditions described above, the magnitudes of forces exerted on partially immersed nanoparticles on the substrate versus the intersurface distance. It is indicated that the active range of each force is so different that the magnitude relation of these forces considerably changes with the intersurface distance.

Figure 5 shows a time history of snapshots of colloidal nanoparticles. Upper picture and lower picture show top view and side view, respectively. At the beginning of the simulation, nanoparticles are randomly located

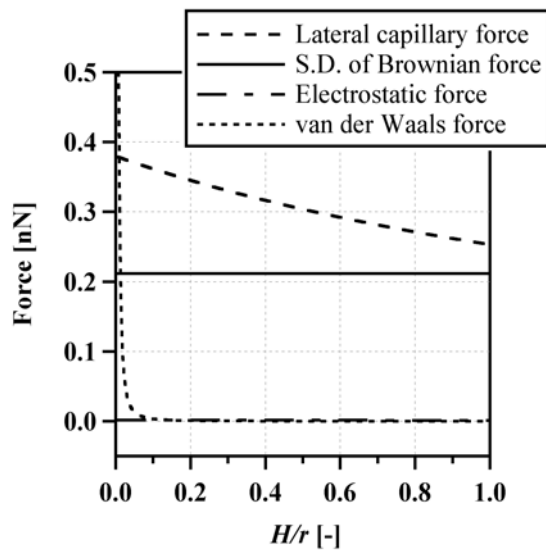


Figure 4. Magnitudes of forces exerted on a nanoparticle ($h/r=1.25$)

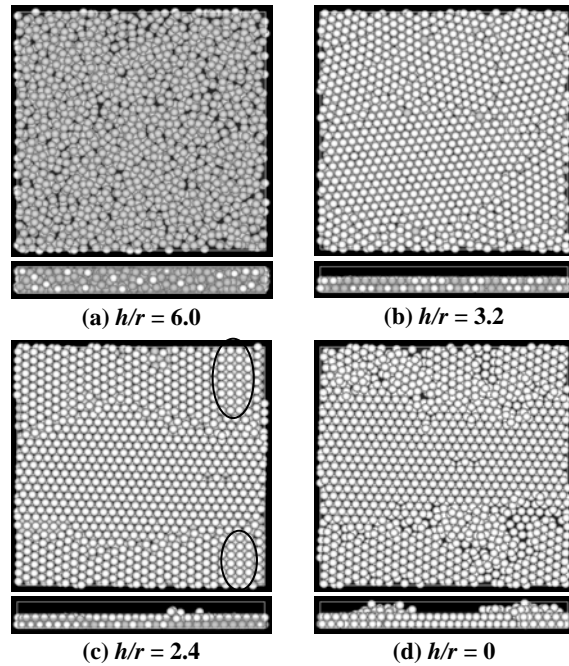


Figure 5. Snapshots of colloidal nanoparticles

in the computational region, as shown in Figure 5(a). The nanoparticles move downward along with the interface, and form a planar crystalline structure due to lateral capillary immersion forces among upper-layered nanoparticles, as shown in Figure 5(b). The capillary forces become stronger as the solvent film gets thinner, and rearrangement of the nanoparticles occurs. Due to the rearrangement, tetragonal arrays of nanoparticles are

generated in the small and some nanoparticles are pushed on to the upper layer, as shown in Figure 5(c). Finally, the nanoparticles form a double layer crystalline structure with some defects and some overflows on the upper layer, as shown in Figure 5(d). Vertical structures of nanoparticles in Figure 10 are illustrated in Figure 11, which shows the probability density distribution of the height of nanoparticle center from the substrate. Although the initial distribution is almost flat, two peaks arise as the double layer forms. The final upper peak is located in $z/r=2.63$, which corresponds to the height of center of the upper-layered spheres in the hexagonally close-packed spheres. The downward displacement of the two peaks at $h/r=2.4$ from the final locations indicates that most nanoparticles are pushed down by the strong vertical capillary force and have compressive strains at the moment.

A three-dimensional structure formation simulator of colloidal nanoparticles during drying was developed. The simulator reproduced a multilayer structure of nanoparticles on a substrate after drying. The process of structure formation was visualized, and vertical and planar structures of nanoparticles were temporally and quantitatively evaluated using the positions of nanoparticles. The simulation result revealed the moment of structure formation and the primary mechanism of structure formation as follows: The upper-layered nanoparticles are subject to the lateral capillary immersion force as they put on the lower-layered nanoparticles on the substrate. The crystallization of the upper-layered nanoparticles causes that of the lower-layered nanoparticles. Future studies by the present simulator may clarify the relationship between process conditions of drying and three-dimensional structures of nanoparticles.

3. Conclusions

There are a lot of examples on self-organization both on process and function. The key to understand self-organization are following. First, we understand the mechanism of self-organization from the physico-chemical point of view. Second, we establish the mathematical equation sets for a special case based on the mechanism. Third, we try to establish the general understanding for self-organization. Then, we can intentionally use self-organization for the functional material design in future.

The self-organization of nanoparticles on a substrate under shear flow and post shear flow, and during drying was studied to obtain the necessary conditions for thin films of highly ordered nanoparticles. The dynamic behavior of nanoparticles during drying was also modeled in 3 dimensions and resulted in a good agreement with experimentals. It is concluded that repulsive forces among particles and between particles and a substrate are preferable to obtain highly ordered nanoparticles.

REFERENCES

- 1) T. Okubo, S.Chujyo, S. Maenosono, and Y. Yamaguchi: Microstructure of Silica Particle monolayer films formed by capillary immersion force, *J. of Nanoparticle Research*, 5, 111-117 (2003)
- 2) M. Fujita and Y. Yamaguchi: Development of Three-Dimensional Structure Formation Simulator of Colloidal Nanoparticles during Drying, *Journal of Chemical Engineering of Japan*, (submitted).
- 3) M. Fujita, H. Nishikawa, T. Okubo and Y. Yamaguchi: Multiscale Simulation of Two-Dimensional Self-Organization of Nanoparticles in Liquid Film, *Jpn. J. Appl. Phys.*, 43, 4434-4442 (2004)